










RESEARCH ARTICLE | JANUARY 07 2025

Multicaloric effect in FeRh, exploiting the thermal hysteresis in a multi-stimuli cycle combining pulsed magnetic field and uniaxial load

Special Collection: [Multicalorics II](#)

F. Scheibel ; N. Shayanfar ; L. Pfeuffer ; T. Gottschall ; S. Dittrich; A. Taubel ; A. Aubert ; I. Radulov ; K. P. Skokov ; O. Gutfleisch 



J. Appl. Phys. 137, 014901 (2025)

<https://doi.org/10.1063/5.0238689>



Articles You May Be Interested In

Demonstration of the multicaloric effect in a laboratory prototype

J. Appl. Phys. (August 2024)

Multicaloric effect in bi-layer multiferroic composites

Appl. Phys. Lett. (November 2015)

Multicaloric strategy to manipulate optimal operating temperature window: An experimental study on $(\text{Ni}_{43}\text{Mn}_{47}\text{Sn}_{10})_{99.5}\text{Tb}_{0.5}$ via a direct method

APL Mater. (November 2023)



Journal of Applied Physics

Special Topics Open for Submissions

[Learn More](#)



Multicaloric effect in FeRh, exploiting the thermal hysteresis in a multi-stimuli cycle combining pulsed magnetic field and uniaxial load

Cite as: J. Appl. Phys. 137, 014901 (2025); doi: 10.1063/5.0238689

Submitted: 13 September 2024 · Accepted: 12 December 2024 ·

Published Online: 7 January 2025



F. Scheibel,^{1,a)} N. Shayanfar,¹ L. Pfeuffer,¹ T. Gottschall,² S. Dittrich,² A. Taubel,¹ A. Aubert,¹ I. Radulov,^{1,3} K. P. Skokov,¹ and O. Gutfleisch^{1,b)}

AFFILIATIONS

¹Functional Materials, Institute of Materials Science, Technical University of Darmstadt, Peter-Grünberg-Straße 16, 64287 Darmstadt, Germany

²Dresden High Magnetic Field Laboratory (HLD-EMFL), Helmholtz-Zentrum Dresden-Rossendorf, 01328 Dresden, Germany

³Fraunhofer Institution for Material Cycles and Resource Strategies IWKS, Hanau, Germany

Note: This paper is part of the special topic, Multicalorics II.

^{a)}Author to whom correspondence should be addressed: franziska.scheibel@tu-darmstadt.de

^{b)}URL: <https://www.mawi.tu-darmstadt.de/fm/>

ABSTRACT

Large magnetocaloric effects can be observed in materials with first-order magneto-structural phase transition. However, materials with large thermal hysteresis show a reduced effect in moderate fields (~ 2 T) because the external field is insufficient to induce a fully reversible transformation. The hysteresis can be overcome or even exploited by applying a second external stimulus. A multi-stimuli test bench has been built to demonstrate the multicaloric effect in FeRh alloy using a pulsed magnetic field up to 9 T and a uniaxial stress of up to 700 MPa. A cyclic multicaloric effect of ± 2.5 K could be observed for a sequential application of a pulsed field of 3 T and a uniaxial stress of 700 MPa. The interplay among external field strength, thermal hysteresis, and the transition width enables the use of pulsed magnetic fields and allows a decoupling of the applied magnetic field and the heat transfer process in the multi-stimuli cycle.

© 2025 Author(s). All article content, except where otherwise noted, is licensed under a Creative Commons Attribution (CC BY) license (<https://creativecommons.org/licenses/by/4.0/>). <https://doi.org/10.1063/5.0238689>

I. INTRODUCTION

Solid-state refrigeration is a promising alternative to conventional vapor-compressing cooling systems and, for several decades, an important research topic.^{1–7} Caloric materials with first-order phase transition can exhibit large caloric effects. However, the inherent thermal hysteresis of first-order phase transition often prevents a fully reversible phase transition for low or moderately single stimulus, which causes a reduction of the caloric effect under cyclic conditions.^{8,9} To obtain a fully reversible phase transition and large magneto-, elasto-, baro-, or electro-caloric effect, high external field strength (magnetic field, stress, pressure, or electric field) is required. Several strategies to reduce thermal hysteresis are investigated,^{10–13} often leading to a reduced caloric effect. In recent

years, the possibility of using multicaloric materials exposed to multiple external stimuli has been investigated in more detail,^{14–17} especially for materials with both magneto- and elastocaloric effects.^{18,19} The magnetoelastic coupling in these multicaloric materials allows a phase transition by multiple external stimuli, magnetic field, and uniaxial load. The research in the area of multicaloric materials is ongoing and requires the optimization of both caloric effects. However, using multicaloric materials also opens the possibility of developing new cooling concepts and overcoming drawbacks for several caloric materials with first-order phase transition. The application of two stimuli is beneficial for broadening the operating temperature span,^{20,21} reducing the effective thermal hysteresis,⁸ and can also be used to reduce the

magnitude of the applied external field.^{18,19} The latest is especially important for elastocaloric materials since a reduction of the applied uniaxial load can significantly increase the cyclic stability of the material. The literature for multicaloric materials often only contains studies on monocoloric effects; multiple caloric effects are rarely investigated. Determining the multicaloric response of a multicaloric material cannot be done by simply adding the corresponding monocoloric effects due to the strong coupling between the different degrees of freedom.²² But, a few multi-stimuli test benches coupling the magneto- and elastocaloric effects have developed in recent years. However, direct measurements of the multicaloric effect or multi-stimuli calorimetry measurements are essential since the transformation phase of the first-order phase transition can vary depending on the different applied stimuli and their specific configurations.²³ Regarding the configuration, different application processes are possible: serial^{21,24} and parallel^{19,21,25} applications of external stimuli or the application of one stimulus keeping the other one constant.^{26,27} The benefit of the serial application is the decoupling of the application of the stimuli and the heat-transfer process.²⁴ In this six-step multi-stimuli cooling cycle, the thermal hysteresis of the multicaloric material is exploited to separate the forward and reverse transformation processes.

Figure 1 shows a serial, non-synergic multi-stimuli cycle using a pulsed magnetic field to induce the first-order magneto-structural transition of a multicaloric material and a uniaxial load to reverse the transition. The thermal hysteresis of the material prevents the reverse phase transformation when the external field/load is removed, and the heat absorption and emission processes can take place without the presence of the stimuli. This decoupling significantly reduces the time the material has to be exposed to the external magnetic field and enables the use of pulsed magnetic fields as the source. Pulsed fields cannot be used in the magnetocaloric cooling cycles or parallel (synergic) multiferroic cooling cycles using the magnetocaloric effect since the heat transfer process is too slow compared to the pulse duration, and the heat transfer process is coupled to the presence of the applied magnetic field. Using a pulsed field also has the advantage that a higher field strength of up to 10 T can be realized, while for single-stimulus or serial multi-stimuli cycles, the magnetic field is limited to a maximum of 2 T since permanent magnets or electromagnets are used for applying the external field.^{21,24} The development of multicaloric measurement devices is important as the cross-coupling of the different subsystems can be investigated, and the use of a high magnetic field and large uniaxial load is beneficial since the caloric properties for a complex first-order phase transition can be investigated to gain a better fundamental understanding of the process.

This study developed a home-built multicaloric test bench with a pulsed-magnetic field and uniaxial stress as external stimuli to determine the multicaloric effect in materials with magneto- and elastocaloric effects. The test bench is designed to enable a sequential application of the external stimuli to realize the six-step multicaloric cooling cycle to exploit the thermal hysteresis. The device is used to determine the reversible multicaloric effect of FeRh, which undergoes a first-order phase transition from the low-temperature antiferromagnetic (AFM) to high-temperature ferromagnetic (FM) phase.

II. EXPERIMENTAL DETAILS

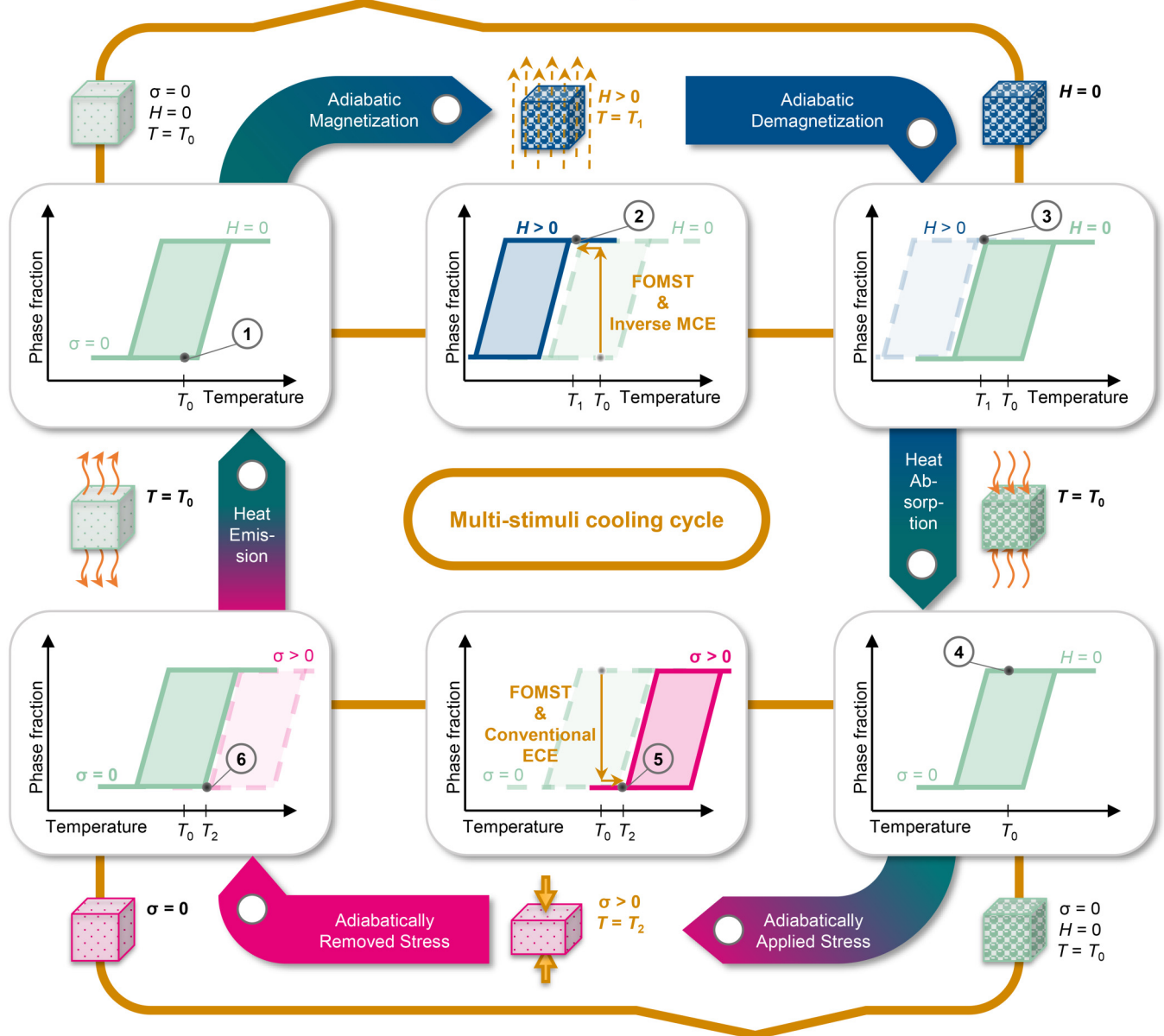
We choose FeRh as a benchmark material to determine the multicaloric effect in the newly developed multicaloric test bench with sequentially applied pulsed magnetic field and uniaxial stress. The FeRh sample was synthesized by arc-melting and subsequent suction casting into a rod with a diameter of 5 mm. The sample was heat-treated at 1273 K for 72 h for homogenization, followed by quenching in water. The chemical composition Fe₅₁Rh₄₉ was determined by energy dispersive x-ray spectroscopy (EDX). For the multicaloric measurements, a cylinder with a height of 10 mm was cut from the center of the rod. The bottom and top surfaces of the cylinder were polished to ensure plane-parallel surfaces.

The temperature-dependent magnetization $M(T)$ measurements were performed in a PPMS (Physical Property Measurement System) with a maximum magnetic field of 14 T. A vibration scanning magnetometer (VSM) was used to determine $M(T)$ under cooling and heating with a rate of 1 K min⁻¹ for the fields of 0.1, 1, 2, 5, and 10 T. The transition temperatures for forward and reverse first-order transitions were determined by the tangent method explained in Ref. 28.

The magnetic-field induced adiabatic temperature change ΔT_{ad} without mechanical load was determined using a purpose-built magnetocaloric test bench with a rotating double Halbach permanent magnet array with a sinusoidal magnetic-field profile and a maximum field of 1.93 T. The temperature change of the sample was obtained by attaching a differential type T thermocouple and ice-water as the temperature reference. A detailed description of the device can be found in Ref. 8 and its supplementary material. The measurements were performed using a discontinuous protocol where the sample was heated up to 310 K and, subsequently, cooled down to 255 K in zero fields. After this heating-cooling cycle, the sample was heated to the start temperature of the ΔT_{ad} measurement. The protocol was used to ensure a defined initial state.

A new multi-stimuli test bench was designed to measure the multicaloric temperature change under the sequential application of a pulsed magnetic field and dynamic uniaxial load. The multi-stimuli test bench is shown in Fig. 2 combining an INSTRON universal testing machine to apply the uniaxial load up to 30 kN and a pulsed-field solenoid to generate a field of up to 9 T. The sample and the solenoid were located within an INSTRON environmental chamber, which controlled the temperature of the experiment. It allowed varying within a temperature range between 250 and 350 K. The pulsed magnetic field was generated by an in-house-developed non-destructive solenoid produced at Dresden High Magnetic Field Laboratory (HLD), a Member of the European Magnetic Field Laboratory (EMFL), Helmholtz-Zentrum Dresden-Rossendorf (HZDR). The field solenoid can generate high magnetic fields up to 9 T with a duration of 2.1 ms and requires no active cooling. A capacitor bank with a maximum voltage of 3 kV was used. The pulse profile and additional information are given in the [supplementary material](#). The uniaxial load was applied via an INSTRON 5967 universal testing machine with a static load cell of maximum 30 kN. The sample was mounted between the upper and the lower punch in the center of the

1. Stimulus: Pulsed magnetic field inducing FOMST from phase 1 → phase 2



2. Stimulus: Uniaxial stress reverses FOMST from phase 2 → phase 1

FIG. 1. Serial multicaloric cooling cycle using a magnetic field and uniaxial load as external stimuli. The thermal hysteresis of the multicaloric material prevents a reverse transformation after the external stimuli are removed, enabling a thermal exchange without applied stimuli. The two individual caloric effects are non-synergic.

solenoid. A type K thermocouple determined the sample temperature, and the pulsed field was determined by a pick-up coil. The time-dependent sample temperature and the induced signal in the pick-up coil were measured using a YOKOGAWA DL850E signal recorder and an oscilloscope. All wires have been twisted to suppress parasitic induction signals.

III. RESULTS AND DISCUSSION

A. First-order phase transition in FeRh

We performed temperature-dependent magnetization measurements $M(T)$ to determine the shift of the first-order magnetostructural phase transition (FOMST) with the externally applied

09 January 2025 10:50:37

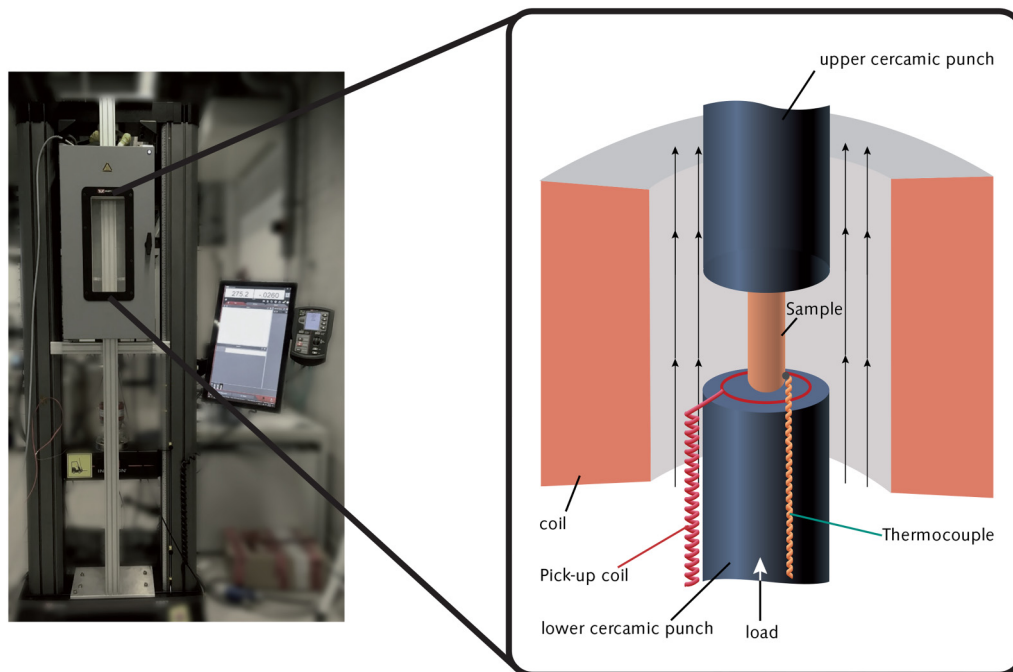


FIG. 2. Multistimuli test bench combines an INSTRON universal testing machine to apply a uniaxial load and a solenoid to generate a pulsed magnetic field. The sample and the solenoid are located within an INSTRON environmental chamber, which controls the set temperature of the experiment.

magnetic field. Figure 3(a) shows the $M(T)$ -curves for the FeRh sample in fields of 0.1, 1, 2, 5, and 10 T. The FOMST from the high-temperature ferromagnetic phase to the low-temperature anti-ferromagnetic phase shifts toward lower temperatures for increasing magnetic field. The start and finish temperatures of the forward ($T_{AFM,start}$ and $T_{AFM,finish}$) and reverse transformations ($T_{FM,start}$ and $T_{FM,finish}$) are shown in Fig. 3(b), the shift of the FOMST is determined by a linear fit of the critical temperatures indicating a shift of -9.0 K T^{-1} for the FM-to-AFM phase transformation and a shift of -9.8 K T^{-1} for the reverse transformation; these values fit the field sensitivities reported in the literature.^{29,30} However, it needs to be considered that the transition temperature and thermal hysteresis are very sensitive to the chemical composition, doping, heat treatment, and external pressure.^{31–39}

The difference in field sensitivity for the forward and reverse transformations leads to an increase of the thermal hysteresis with increasing field, namely, 24 K in 0.1 T and 32 K in 10 T. This effect is known from the literature and relates to the increase of ferromagnetic contribution at lower temperatures.⁴⁰ A transition width of about 8 K can be estimated by $|T_{AFM,start} - T_{AFM,finish}|$ and $|T_{FM,start} - T_{FM,finish}|$. Due to the strongly flattened transformation at the beginning and end of the transformation, this estimate is more of a minimum value of the transformation width. If the flattening curves at the beginning and end of the transformation are considered, a transformation width of 25–35 K can certainly be assumed. In this case, the transition width and the thermal hysteresis are similar; this

aspect will be important in the further discussion of the caloric effect in a pulsed magnetic field.

B. Caloric effect using single stimulus: Magnetic field

The magnetocaloric effect for a single stimulus is determined by direct measurements of the adiabatic temperature change ΔT_{ad} in an applied field of 1.9 T. The magnetic-field profile of the rotating nested Halbach array is shown in Fig. 4(a). ΔT_{ad} measurements are determined in a temperature interval between 258 and 308 K, using the discontinuous measurement protocol (see Sec. II).

Figure 4(b) shows the field-dependent ΔT_{ad} for the temperatures closest to $T_{FM,start}$ at 0 T. The drop of ΔT_{ad} appears after the critical field is reached. The critical field depends on the initial temperature where the measurement is started and increases for the decreasing initial temperature. With the increasing field, much of the FeRh AFM phase is transformed into the FM phase; however, due to the large transformation width, a complete transformation cannot be induced by a field of 1.9 T. The highest phase fraction and, therefore, the highest $|\Delta T_{ad}|$ can be induced at an initial temperature of 289.89 K, which is closest to $T_{FM,start}$ at 0 T. For 291.86 K, a lower $|\Delta T_{ad}|$ is determined since this initial temperature is higher than $T_{FM,start}$ at 0 T and a certain phase fraction is already transformed, and the applied magnetic field can only induce the remaining phase fraction. For demagnetization, $|\Delta T_{ad}|$ decreases further due to the conventional magnetocaloric effect of the FM phase. After the field is removed, the temperature of the FeRh

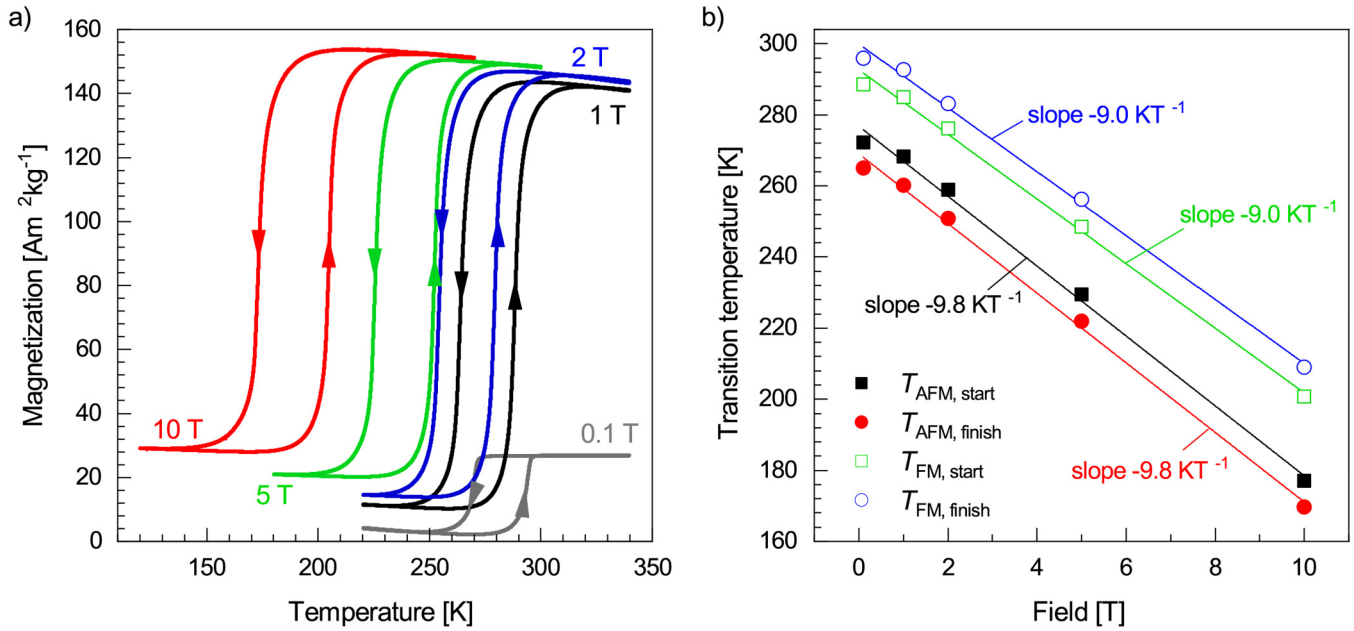


FIG. 3. (a) Temperature-dependent magnetization of FeRh for different fields. (b) Start and finish temperatures of FOMST as a function of the applied field.

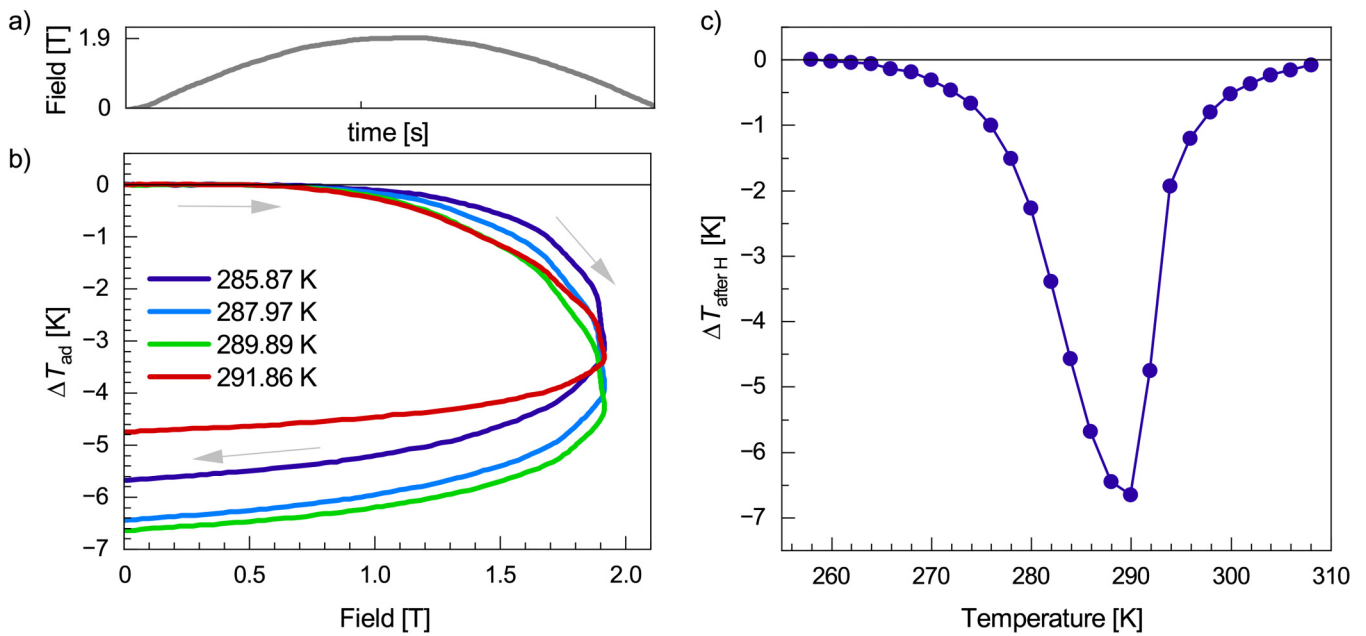


FIG. 4. (a) Magnetic-field profile of the nested Halbach magnet. (b) ΔT_{ad} as a function of applied field for different stating temperatures. (c) $\Delta T_{\text{after H}}$ as a function of the starting temperature.

09 January 2025 10:50:37

sample decreases between -4.75 and -6.73 K, depending on the start temperature. The largest decrease of the temperature difference before and after applying the magnetic field $\Delta T_{\text{after } H}$ is observed when the starting temperature is equal to $T_{\text{FM},\text{start}}$. The fact that the largest $|\Delta T_{\text{ad}}|$ is observed after the magnetic field is removed to 0 proves that the transformation is irreversible due to the thermal hysteresis. Figure 4(c) shows the temperature difference before and after applying the magnetic field $\Delta T_{\text{after } H}$ as a function of the initial temperature. The largest $|\Delta T_{\text{after } H}|$ can be observed in the vicinity of $T_{\text{FM},\text{start}}$ at 0 T. The decrease of $|\Delta T_{\text{after } H}|$ above and below $T_{\text{FM},\text{start}}$ at 0 T is related to the insufficient applied magnetic-field strength to induce a full transformation and the already partially transformed sample, respectively. For temperatures above $T_{\text{FM},\text{finish}}$ at 0 T, no transformation can be induced at all.

The ΔT_{ad} measurement in the rotating nested Halbach magnet shows that the demagnetization of the sample does not reverse the transformation. This is important for the adiabatic measurement in the pulsed magnetic field since the field duration of the pulsed magnetic field is too fast for the response time of the thermocouple. Therefore, only the temperature difference before and after the pulsed magnetic field is determined, and a reverse transformation during demagnetization has to be prevented. The magnetic-field strengths for a complete irreversible and reversible phase transition can be estimated from the thermal hysteresis, the transformation temperature, and the determined shift of the phase transition in the field, measured in Fig. 3. The first step is a complete transformation of the material by applying the magnetic field $H_{\text{full Trans}}$. The required field depends on the transition width $|T_{\text{FM},\text{start}} - T_{\text{FM},\text{finish}}|$ and the shift of the transition temperature with applied field $dT_{\text{FM},j}/dH$ ($j=\text{start, finish}$)

$$H_{\text{full Trans}} = \frac{|T_{\text{FM},\text{start}} - T_{\text{FM},\text{finish}}|}{|dT_{\text{FM},j}/dH|}. \quad (1)$$

For the FeRh sample, $|T_{\text{FM},\text{start}} - T_{\text{FM},\text{finish}}|$ is 25–35 K and $dT_{\text{FM},j}/dH$ is -9.0 K T^{-1} , and a complete transformation would

require an external field with a strength between 2.8 and 3.9 T. In the second step, the thermal hysteresis ΔT_{hyst} prevents a reversible transformation when the field is removed. If $\Delta T_{\text{hyst}} \geq H_{\text{full Trans}} \cdot dT_{\text{FM},\text{start}}/dH$, the transformation would be entirely irreversible. For $0 < \Delta T_{\text{hyst}} < H_{\text{full Trans}} \cdot dT_{\text{FM},\text{start}}/dH$, the removal of the field would lead to a partially reversed transformation. To induce a fully reversible transformation, additional field strength $H_{\text{pass hyst}}$ has to be applied to overcome ΔT_{hyst}

$$H_{\text{pass hyst}} = \frac{\Delta T_{\text{hyst}}}{|dT_{\text{FM},\text{start}}/dH|}. \quad (2)$$

For the FeRh sample, ΔT_{hyst} is 24–32 K and $dT_{\text{FM},j}/dH$ is -9.0 K T^{-1} ; therefore, $H_{\text{pass hyst}}$ is 2.7–3.6 T. A complete reversible transformation, therefore, would require an applied field $H_{\text{full Trans}} + H_{\text{pass hyst}}$ with a field strength of 5.5–7.5 T.

Therefore, a field strength of 3 T is used for the temperature change measurement in the pulsed magnetic field to ensure full transformation during magnetization and exclude the reverse transformation during demagnetization. Figure 5(a) shows the time-dependent temperature change $T - T_{t=0}$ for different starting temperatures 275.6, 280.6, 285.3, 290.2, and 295.9 K. The pulsed field of 3 T is applied after 0.1 s, and the gray area marks the pulse duration. The temperature of the sample decreases as soon as the field is applied, and the AFM-to-FM phase transition is induced. However, a delay in the temperature response is observed because the thermal coupling between the sample and the thermocouple attached to the sample surface is limited. This leads to a delay in the temperature measurement by approximately 0.2 s. After 0.3 s, $T - T_{t=0}$ is constant and both the sample and thermocouple reach thermal equilibrium.

The $\Delta T_{\text{after } H}$ as a function of the initial temperature is shown in Fig. 5(c). Compared with $\Delta T_{\text{after } H}$ determined in 1.9 T, the temperature change in the 3 T pulsed magnetic field reaches a minimum value of -7.5 K in the temperature range between 285

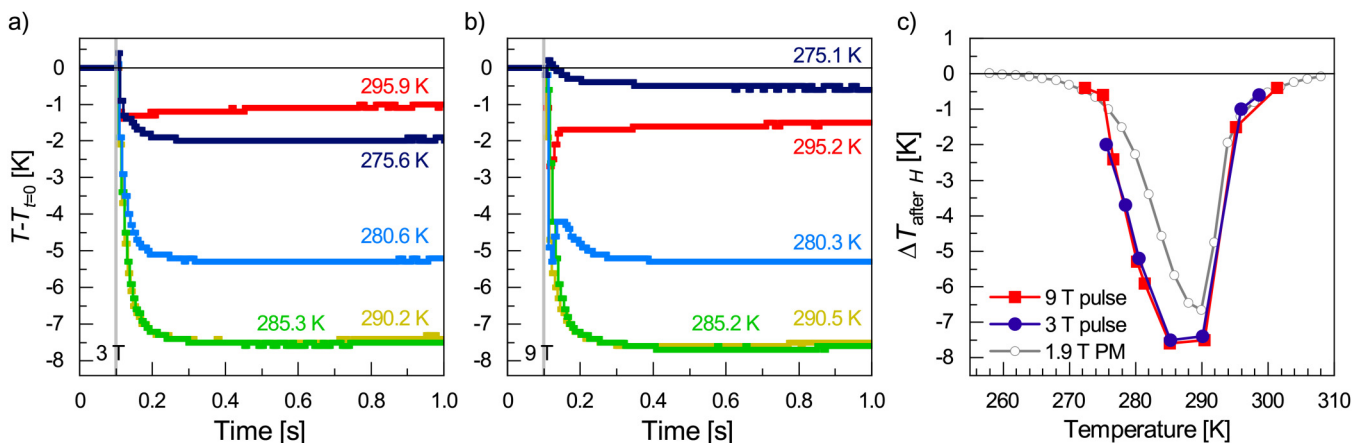


FIG. 5. Temperature change $T - T_{t=0}$ as a function of time for (a) 3 T and (b) 9 T field pulse for different starting temperatures. The gray area shows the time duration of the pulsed field. (c) $\Delta T_{\text{after } H}$ as a function of starting temperature for 3 and 9 T pulsed fields and 1.9 T Halbach magnet.

09 January 2025 10:50:37

and 290 K. This indicates that a field of 3 T can induce a complete transformation. For temperatures higher than 290 K, the sample is already partially transformed before the pulsed field, leading to a lower $|\Delta T_{\text{after } H}|$. For temperatures below 285 K, the field strength of 3 T is insufficient to induce a complete transformation. As the critical field to induce the phase transformation increases with the decreasing initial temperature, $|\Delta T_{\text{after } H}|$ exhibits a reduction when the initial temperature is lower. However, compared to the field of 1.9 T, the pulsed field of 3 T can induce a transformation at a lower temperature.

For 3 T, a complete and irreversible transformation is observed, and a further increase in the magnetic field strength will not lead to a higher temperature change after the pulsed field. To confirm this, the temperature measurements before and after the pulsed magnetic field are also determined for a field strength of 9 T. Figure 5(b) shows $\Delta T_{\text{after } H}$ for the 9 T pulses. Similar starting temperatures, as for the 3 T pulses, are chosen for a better comparison. $\Delta T_{\text{after } H}$ of 9 and 3 T are comparable. One exception is the temperature change for 275.6 K [Fig. 5(a)] and 275.1 K [Fig. 5(b)], but the slight variation of the initial temperature can explain this. $\Delta T_{\text{after } H}$ for 9 T as a function of the initial temperature is shown in Fig. 5(c). As assumed, the $\Delta T_{\text{after } H}(T)$ -curve for 3 and 9 T overlap. A maximum temperature change before and after the pulsed field of -7.5 K is determined for a start temperature between 285 and 290 K. Similar $\Delta T_{\text{after } H}$ values are also found in the literature.^{40,41} However, in the literature, mainly the maximum adiabatic temperature change $|\Delta T_{\text{ad}}|$ is determined, while in this study, the temperature after the pulsed field is determined. The max. $|\Delta T_{\text{ad}}|$ values are determined at the maximum field,^{18,26,40} and this excluded the

effect of a reverse transformation during demagnetization. Since the effect is not excluded for $\Delta T_{\text{after } H}$, the max. $\Delta T_{\text{ad}}(T)$ -curve in the literature and the $\Delta T_{\text{after } H}(T)$ -curve in this study slightly vary. For the $\Delta T_{\text{after } H}(T)$ -curve, no broadening of the peak toward the lower temperature is observed for 9 T, in comparison to the $\Delta T_{\text{after } H}(T)$ -curve in 3 T. Such a broadening is only observed for the $\Delta T_{\text{ad}}(T)$ -curve determined at the maximum field excluding the reverse transformation, which is, for example, shown in Refs. 18, 26, 40, and 42.

C. Multicaloric effect using two stimuli: Magnetic field and uniaxial load

To determine the multicaloric effect, a sequential application of a 3 T field and a uniaxial load of 600 MPa is applied for several start temperatures using the newly developed multi-stimuli test bench described in Sec. II. The subsequent discontinuous heating-cooling protocol is used to set the start temperature, and a sequential application of three field pulses and two stress applications is carried out. Figure 6(a) shows schematically the sequential multi-stimuli cycle; both stimuli are applied under adiabatic conditions. The temperature change as a function of time for a start temperature of 280 K is shown in Fig. 6(b). The first applied field pulse led to a field-induced AFM-to-FM transformation and a magneto-caloric effect of -4.7 K. After the pulse, the sample warms until the initial start temperature is reached. After the sample has reached the thermal equilibrium, the first application of uniaxial stress is performed, and the sample undergoes the reverse FM-to-AFM transformation with an elastocaloric effect of 2.4 K. The sequential

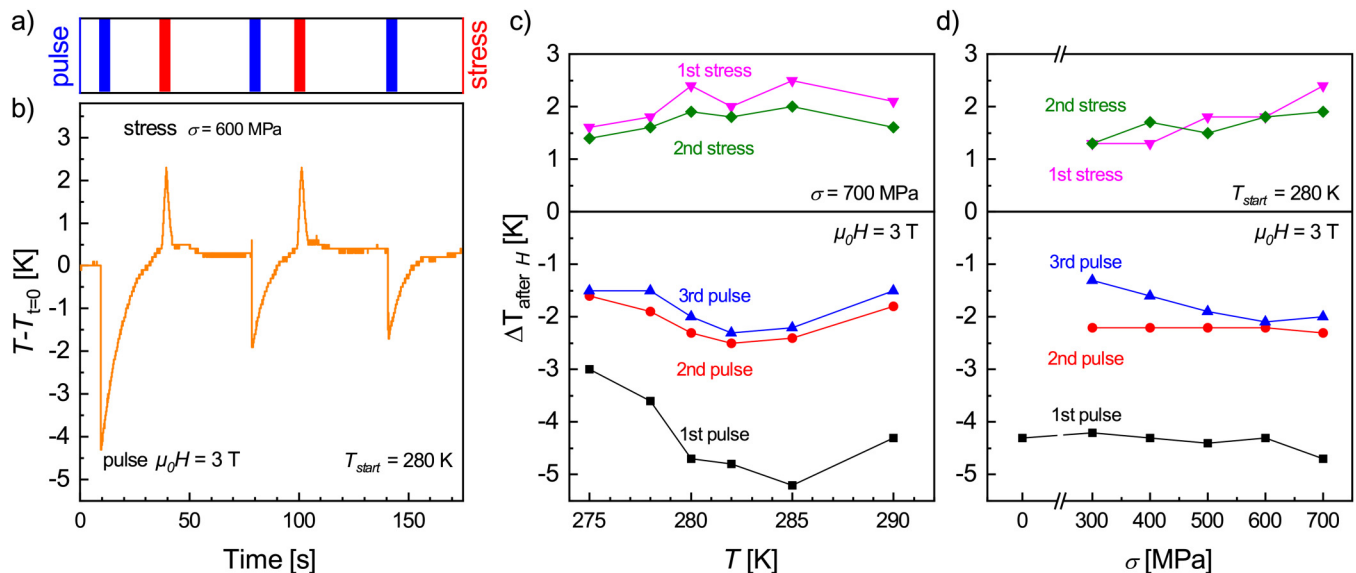


FIG. 6. (a) Schematics of the sequential application of a pulsed field and uniaxial stress for the sequential multi-stimuli cycle. (b) Temperature change $T - T_{i=0}$ as a function of time for the sequential application of a 3 T pulsed field and 700 MPa uniaxial stress. (c) Maximum temperature change after the adiabatically applied stimuli for each pulsed field and applied stress as a function of the starting temperatures. (d) Maximum temperature change after multiple stimuli at a starting temperature of 280 K, a 3 T pulsed field, and different uniaxial stresses.

application of pulsed-field and uniaxial stress is repeated with, for the second iteration of applied field and stress, a magneto- and elastocaloric effect of -2.3 and 1.9 K is induced, respectively. A third pulsed field is applied, leading to a magnetocaloric effect of -2.0 K.

This sequential application of multi-stimuli is performed for different start temperatures between 275 and 290 K for an applied field of 3 T and a uniaxial stress of 700 MPa. Figure 6(c) shows the temperature change after different stimuli. For all start temperatures, a reduction of the magnetocaloric effect after the first applied pulsed field is present, indicating that a part of the sample is not transformed by the second stimulus (first stress application). During further cycling, the magneto- and elastocaloric effects saturate, and only a minor reduction of the caloric effect can be determined between the second and third pulsed fields and the first and second stress applications. Multicaloric measurements of ten cycles show that the multicaloric effect saturates after the second multi-stimuli cycle; more information is provided in the [supplementary material](#). The reduction of the magnetocaloric effect after the first pulse field application is also present for multicaloric measurements at different uniaxial stresses. Figure 6(d) shows the magneto- and elastocaloric effects for a multi-stimuli cycle at 280 K using a pulsed field of 3 T and a uniaxial stress between 0 and 700 MPa. In addition to the reduction of the magnetocaloric effect after the first field application, an increase in the elastocaloric effect with increasing applied stress can be observed, indicating that with increasing stress, a higher phase fraction of austenite can be transformed into the low-temperature AFM phase. Meanwhile, an increase in the elastocaloric effect with increasing applied stress is expected. The reason for the reduction of the multicaloric effect after the first field application requires further research. However, one reason for this reduction can be a difference in the low-temperature AFM phase before the first and second pulsed field applications. Before the first field pulse, the discontinuous heating-cooling protocol was used to reach the starting temperature of the measurement; the low-temperature AFM phase is thermally induced without the pressure of stress or field. For the second field application, the AFM phase is induced by applying stress, which can result in a microstructural configuration different from that of the thermally induced one. The stabilization of the multicaloric effect after the third cycle is comparable to a minor loop, which is observed in caloric cycles with only one stimulus.⁴³

The difference between a minor loop in a sequential multi-stimuli cycle and a single-stimulus cycle is that an alternation of the pulsed magnetic field and uniaxial stress must always be applied. In case the field is applied twice, no phase transformation will be induced during the second application of the field, and no caloric effect will be observed. Such a sequence with two field pulses directly after each other is shown in the [supplementary material](#). To regain a caloric effect for the pulsed field, the transformation has to be reversed by applying uniaxial stress. This shows that the thermal hysteresis prevents a reverse transformation after the pulsed field, and a cyclic caloric effect can only be induced by the combination of both stimuli, pulsed field, and uniaxial stress.

IV. CONCLUSION

This study shows that a sequential application of a pulsed magnetic field and uniaxial stress leads to a reversible multicaloric effect in FeRh, despite large thermal hysteresis, which would prevent a reversible magnetocaloric effect for a single-stimulus cycle. The benefit of the multicaloric cycle lies in the exploitation of the thermal hysteresis, which makes it also possible to use pulsed magnetic fields as magnetic stimuli and gain a reversible caloric effect for materials with the first-order transition. However, the combination of thermal hysteresis, sensitivity of phase transformation with the applied stimulus, and the transition width has to be properly adjusted with the strength of the applied stimuli to ensure a complete phase transformation and exclude a reverse transformation when the stimulus is removed. The used FeRh sample with a thermal hysteresis of ~ 28 K and a transition width of ~ 30 K fulfill this requirement, and a pulsed-field of 3 T leads to a complete but irreversible transition, and a magnetocaloric effect of -7.5 K in the vicinity of the first-order transition. The development of the multi-stimuli test bench opens up new possibilities for determining the multicaloric effect and is, to the best of our knowledge, the only test bench enabling a sequential application of a pulsed magnetic field and uniaxial stress.

SUPPLEMENTARY MATERIAL

The [supplementary material](#) includes further information on the magnetic-field profile of pulsed-field solenoid, the cyclic multicaloric effect for multi-stimuli, and the proof of concept of exploiting the thermal hysteresis by the six-step multi-stimuli cycle.

ACKNOWLEDGMENTS

This work is supported by funding from the European Research Council (ERC) under the European Union's Horizon 2020 research and innovation program (Grant No. 743116—Cool Innov), the Deutsche Forschungsgemeinschaft (DFG) CRC/TRR 270 “HoMMage” (Project-ID 405553726-TRR 270), BEsT (Project-ID 456263705), and the HLD at HZDR, a member of the European Magnetic Field Laboratory (EMFL).

AUTHOR DECLARATIONS

Conflict of Interest

The authors have no conflicts to disclose.

Author Contributions

F. Scheibel: Conceptualization (equal); Data curation (equal); Formal analysis (equal); Investigation (equal); Methodology (equal); Project administration (equal); Supervision (equal); Validation (equal); Writing – original draft (lead); Writing – review & editing (lead). **N. Shayanfar:** Conceptualization (equal); Investigation (lead); Methodology (lead); Validation (equal); Writing – review & editing (equal). **L. Pfeuffer:** Conceptualization (equal); Data curation (equal); Formal analysis (lead); Investigation (lead); Methodology (equal); Validation (equal); Writing – original draft (supporting); Writing – review & editing (equal). **T. Gottschall:** Conceptualization (supporting); Data curation (supporting); Funding acquisition

(supporting); Investigation (supporting); Methodology (supporting); Resources (equal); Validation (supporting); Writing – original draft (supporting); Writing – review & editing (equal). **S. Dittrich:** Methodology (supporting); Resources (supporting); Validation (supporting). **A. Taubel:** Conceptualization (equal); Data curation (equal); Formal analysis (supporting); Investigation (equal); Methodology (supporting); Project administration (supporting); Resources (equal); Supervision (supporting); Validation (supporting); Writing – review & editing (supporting). **A. Aubert:** Formal analysis (supporting); Investigation (supporting); Resources (equal); Writing – review & editing (equal). **I. Radulov:** Conceptualization (equal); Methodology (equal); Resources (supporting); Validation (supporting); Visualization (supporting); Writing – review & editing (supporting). **K. P. Skokov:** Conceptualization (supporting); Formal analysis (supporting); Methodology (equal); Project administration (supporting); Supervision (supporting); Writing – review & editing (supporting). **O. Gutfleisch:** Conceptualization (equal); Funding acquisition (lead); Methodology (supporting); Project administration (lead); Resources (lead); Supervision (equal); Writing – review & editing (supporting).

DATA AVAILABILITY

The data that support the findings of this study are available from the corresponding author upon reasonable request.

REFERENCES

- ¹I. Takeuchi and K. Sandeman, “Solid-state cooling with caloric materials,” *Phys. Today* **68**, 48–54 (2015).
- ²S. Qian, Y. Geng, Y. Wang, J. Ling, Y. Hwang, R. Radermacher, I. Takeuchi, and J. Cui, “A review of elastocaloric cooling: Materials, cycles and system integrations,” *Int. J. Refrig.* **64**, 1–19 (2016).
- ³O. Gutfleisch, M. A. Willard, E. Bruck, C. H. Chen, S. G. Sankar, and J. P. Liu, “Magnetic materials and devices for the 21st century: Stronger, lighter, and more energy efficient,” *Adv. Mater.* **23**, 821–842 (2011).
- ⁴L. Mañosa and A. Planes, “Solid-state cooling by stress: A perspective,” *Appl. Phys. Lett.* **116**, 050501 (2020).
- ⁵A. Kitanovski, “Energy applications of magnetocaloric materials,” *Adv. Energy Mater.* **10**, 1903741 (2020).
- ⁶X. Moya and N. D. Mathur, “Caloric materials for cooling and heating,” *Science* **370**, 797–803 (2020).
- ⁷A. Waske, M. E. Gruner, T. Gottschall, and O. Gutfleisch, “Magnetocaloric materials for refrigeration near room temperature,” *MRS Bull.* **43**, 269–273 (2018).
- ⁸J. Liu, T. Gottschall, K. P. Skokov, J. D. Moore, and O. Gutfleisch, “Giant magnetocaloric effect driven by structural transitions,” *Nat. Mater.* **11**, 620–626 (2012).
- ⁹I. Titov, M. Acet, M. Farle, D. González-Alonso, L. Mañosa, A. Planes, and T. Krenke, “Hysteresis effects in the inverse magnetocaloric effect in martensitic Ni-Mn-In and Ni-Mn-Sn,” *J. Appl. Phys.* **112**, 073914 (2012).
- ¹⁰J. Y. Law, L. M. Moreno-Ramírez, Á. Díaz-García, and V. Franco, “Current perspective in magnetocaloric materials research,” *J. Appl. Phys.* **133**, 040903 (2023).
- ¹¹F. Scheibel, T. Gottschall, A. Taubel, M. Fries, K. P. Skokov, A. Terwey, W. Keune, K. Ollefs, H. Wende, M. Farle, M. Acet, O. Gutfleisch, and M. E. Gruner, “Hysteresis design of magnetocaloric materials—from basic mechanisms to applications,” *Energy Technol.* **6**, 1397–1428 (2018).
- ¹²Ö. Çakır and M. Acet, “Adiabatic temperature change around coinciding first and second order magnetic transitions in $\text{Mn}_3\text{Ga}(\text{C}_{0.85}\text{N}_{0.15})$,” *J. Magn. Magn. Mater.* **344**, 207–210 (2013).
- ¹³L. M. Moreno-Ramírez and V. Franco, “Reversibility of the magnetocaloric effect in the bean-rodbell model,” *Magnetochemistry* **7**, 60 (2021).
- ¹⁴H. Hou, S. Qian, and I. Takeuchi, “Materials, physics and systems for multicaloric cooling,” *Nat. Rev. Mater.* **7**, 633–652 (2022).
- ¹⁵A. Gràcia-Condal, A. Planes, L. Mañosa, Z. Wei, J. Guo, D. Soto-Parra, and J. Liu, “Magnetic and structural entropy contributions to the multicaloric effects in Ni-Mn-Ga-Cu,” *Phys. Rev. Mater.* **6**, 084403 (2022).
- ¹⁶Y. Liu, L. C. Phillips, R. Mattana, M. Bibes, A. Barthélémy, and B. Dkhil, “Large reversible caloric effect in FeRh thin films via a dual-stimulus multicaloric cycle,” *Nat. Commun.* **7**, 11614 (2016).
- ¹⁷E. Stern-Taulats, T. Castán, A. Planes, L. H. Lewis, R. Barua, S. Pramanick, S. Majumdar, and L. Mañosa, “Giant multicaloric response of bulk $\text{Fe}_{49}\text{Rh}_{51}$,” *Phys. Rev. B* **95**, 104424 (2017).
- ¹⁸L. Pfeuffer, A. Gràcia-Condal, T. Gottschall, D. Koch, T. Faske, E. Bruder, J. Lemke, A. Taubel, S. Ener, F. Scheibel, K. Durst, K. P. Skokov, L. Mañosa, A. Planes, and O. Gutfleisch, “Influence of microstructure on the application of Ni-Mn-In Heusler compounds for multicaloric cooling using magnetic field and uniaxial stress,” *Acta Mater.* **217**, 117157 (2021).
- ¹⁹Z. Yu, Y. Liu, Y. Liang, K. Qiao, K. Long, H. Chen, L. Xie, C. Xu, P. Ren, S. V. Taskaev, and H. Zhang, “Multi-field synergistic regulation enhanced multicaloric effect in all-d-metal $\text{Ni}_{37}\text{Co}_{13}\text{Mn}_{35}\text{Ti}_{15}$ alloy,” *J. Alloys Compd.* **976**, 173079 (2024).
- ²⁰Y. Qu, D. Cong, S. Li, W. Gui, Z. Nie, M. Zhang, Y. Ren, and Y. Wang, “Simultaneously achieved large reversible elastocaloric and magnetocaloric effects and their coupling in a magnetic shape memory alloy,” *Acta Mater.* **151**, 41–55 (2018).
- ²¹A. Czernuszewicz, J. Kaleta, and D. Lewandowski, “Multicaloric effect: Toward a breakthrough in cooling technology,” *Energy Convers. Manage.* **178**, 335–342 (2018).
- ²²L. Mañosa, E. Stern-Taulats, A. Gràcia-Condal, and A. Planes, “Cross-coupling contribution to the isothermal entropy change in multicaloric materials,” *J. Phys.: Energy* **5**, 024016 (2023).
- ²³A. Gràcia-Condal, T. Gottschall, L. Pfeuffer, O. Gutfleisch, A. Planes, and L. Mañosa, “Multicaloric effects in metamagnetic Heusler Ni-Mn-In under uniaxial stress and magnetic field,” *Appl. Phys. Rev.* **7**, 041406 (2020).
- ²⁴T. Gottschall, A. Gràcia-Condal, M. Fries, A. Taubel, L. Pfeuffer, L. Mañosa, A. Planes, K. P. Skokov, and O. Gutfleisch, “A multicaloric cooling cycle that exploits thermal hysteresis,” *Nat. Mater.* **17**, 929–934 (2018).
- ²⁵A. Amirov and D. Samsonov, “Demonstration of the multicaloric effect in a laboratory prototype,” *J. Appl. Phys.* **136**, 053902 (2024).
- ²⁶T. Gottschall, E. Bykov, A. Gràcia-Condal, B. Beckmann, A. Taubel, L. Pfeuffer, O. Gutfleisch, L. Mañosa, A. Planes, Y. Skourski, and J. Wosnitzer, “Advanced characterization of multicaloric materials in pulsed magnetic fields,” *J. Appl. Phys.* **127**, 185107 (2020).
- ²⁷H. Qian, J. Guo, Z. Wei, and J. Liu, “Multicaloric effect in synergic magnetostructural phase transformation Ni-Mn-Ga-In alloys,” *Phys. Rev. Mater.* **6**, 054401 (2022).
- ²⁸A. Taubel, T. Gottschall, M. Fries, S. Riegg, C. Soon, K. P. Skokov, and O. Gutfleisch, “A comparative study on the magnetocaloric properties of Ni-Mn-X(-Co) Heusler alloys,” *Phys. Status Solidi B* **255**, 1700331 (2018).
- ²⁹A. B. Batdalov, A. M. Aliev, L. N. Khanov, A. P. Kamantsev, A. V. Mashirov, V. V. Koledov, and V. G. Shavrov, “Specific heat, electrical resistivity, and magnetocaloric study of phase transition in $\text{Fe}_{48}\text{Rh}_{52}$ alloy,” *J. Appl. Phys.* **128**, 013902 (2020).
- ³⁰A. Aubert, K. Skokov, G. Gomez, A. Chirkova, I. Radulov, F. Wilhelm, A. Rogalev, H. Wende, O. Gutfleisch, and K. Ollefs, “Simultaneous multi-property probing during magneto-structural phase transitions: An element-specific and macroscopic hysteresis characterization at ID12 of the ESRF,” *IEEE Trans. Instrum. Meas.* **71**, 1–9 (2022).
- ³¹R. Barua, F. Jiménez-Villacorta, and L. H. Lewis, “Towards tailoring the magnetocaloric response in FeRh-based ternary compounds,” *J. Appl. Phys.* **115**, 17A903 (2014).
- ³²A. S. Komlev, R. A. Makarin, K. P. Skokov, A. M. Chirkova, R. R. Gimaev, V. I. Zverev, N. V. Baranov, and N. S. Perov, “Tuning magnetocaloric effect in

- ternary FeRh-based alloys by slight doping,” *Metall. Mater. Trans. A* **54**, 3683–3690 (2023).
- ³³M. Annaorazov, K. Asatryan, G. Myaligulyev, S. Nikitin, A. Tishin, and A. Tyurin, “Alloys of the FeRh system as a new class of working material for magnetic refrigerators,” *Cryogenics* **32**, 867–872 (1992).
- ³⁴R. Barua, I. McDonald, F. Jiménez-Villacorta, D. Heiman, and L. Lewis, “Multivariable tuning of the magnetostructural response of a Ni-modified FeRh compound,” *J. Alloys Compd.* **689**, 1044–1050 (2016).
- ³⁵H. B. Tran, T. Fukushima, H. Momida, K. Sato, Y. Makino, and T. Oguchi, “Direct and inverse magnetocaloric effects in FeRh alloy,” *J. Alloys Compd.* **926**, 166718 (2022).
- ³⁶A. Chirkova, K. Skokov, L. Schultz, N. Baranov, O. Gutfleisch, and T. Woodcock, “Giant adiabatic temperature change in FeRh alloys evidenced by direct measurements under cyclic conditions,” *Acta Mater.* **106**, 15–21 (2016).
- ³⁷C. Sánchez-Valdés, R. Gimaev, M. López-Cruz, J. Sánchez Llamazares, V. Zverev, A. Tishin, A. Carvalho, D. Aguiar, Y. Mudryk, and V. Pecharsky, “The effect of cooling rate on magnetothermal properties of Fe₄₉Rh₅₁,” *J. Magn. Mater.* **498**, 166130 (2020).
- ³⁸L. H. Lewis, C. H. Marrows, and S. Langridge, “Coupled magnetic, structural, and electronic phase transitions in FeRh,” *J. Phys. D: Appl. Phys.* **49**, 323002 (2016).
- ³⁹A. Aubert, K. Skokov, A. Rogalev, A. Chirkova, B. Beckmann, F. Maccari, E. Dilmieva, F. Wilhelm, V. Nassif, L. V. B. Diop, E. Bruder, J. Löfstrand, D. Primetzhofner, M. Sahlberg, E. Adabifiroozjaei, L. Molina-Luna, G. Gomez, B. Eggert, K. Ollefs, H. Wende, and O. Gutfleisch, “Residual ferromagnetic regions affecting the first-order phase transition in off-stoichiometric Fe-Rh,” *ACS Appl. Mater. Interfaces* **16**, 62358–62370 (2024).
- ⁴⁰A. M. Chirkova, K. P. Skokov, Y. Skourski, F. Scheibel, A. Y. Karpenkov, A. S. Volegov, N. V. Baranov, K. Nielsch, L. Schultz, K.-H. Müller, T. G. Woodcock, and O. Gutfleisch, “Magnetocaloric properties and specifics of the hysteresis at the first-order metamagnetic transition in Ni-doped FeRh,” *Phys. Rev. Mater.* **5**, 064412 (2021).
- ⁴¹A. A. Amirov, F. Cugini, A. P. Kamantsev, T. Gottschall, M. Solzi, A. M. Aliev, Yu. I. Spichkin, V. V. Koledov, and V. G. Shavrov, “Direct measurements of the magnetocaloric effect of Fe₄₉Rh₅₁ using the mirage effect,” *J. Appl. Phys.* **127**, 233905 (2020).
- ⁴²M. P. Annaorazov, S. A. Nikitin, A. L. Tyurin, K. A. Asatryan, and A. Kh. Dovletov, “Anomalously high entropy change in FeRh alloy,” *J. Appl. Phys.* **79**, 1689–1695 (1996).
- ⁴³T. Gottschall, K. P. Skokov, B. Frincu, and O. Gutfleisch, “Large reversible magnetocaloric effect in Ni-Mn-In-Co,” *Appl. Phys. Lett.* **106**, 021901 (2015).